Discovery of ciliary G protein-coupled receptors regulating pancreatic islet insulin and glucagon secretion

Chien-Ting Wu,[1] Keren I. Hilgendorf,[1,2] Romina J. Bevacqua,[3] Yan Hang,[3,4] Janos Demeter,[1] Seung K. Kim,[3,4,5,7] and Peter K. Jackson[1,4,5,7]

[1]Baxter Laboratory, Department of Microbiology and Immunology, Stanford University School of Medicine, Stanford, California 94305, USA; [2]Department of Biochemistry, University of Utah School of Medicine, Salt Lake City, Utah 84112, USA; [3]Department of Developmental Biology, Stanford University School of Medicine, Stanford, California 94305, USA; [4]Stanford Diabetes Research Center, Stanford University School of Medicine, Stanford, California 94305, USA; [5]Department of Medicine, Stanford University, Stanford, California 94305, USA; [6]Department of Pathology, Stanford University, Stanford, California 94305, USA

Multiple G protein-coupled receptors (GPCRs) are expressed in pancreatic islet cells, but the majority have unknown functions. We observed specific GPCRs localized to primary cilia, a prominent signaling organelle, in pancreatic α and β cells. Loss of cilia disrupts β-cell endocrine function, but the molecular drivers are unknown. Using functional expression, we identified multiple GPCRs localized to cilia in mouse and human islet α and β cells, including FFAR4, PTGER4, ADRB2, KISS1R, and P2RY14. Free fatty acid receptor 4 (FFAR4) and prostaglandin E receptor 4 (PTGER4) agonists stimulate ciliary cAMP signaling and promote glucagon and insulin secretion by α- and β-cell lines and by mouse and human islets. Transport of GPCRs to primary cilia requires TULP3, whose knockdown in primary human and mouse islets relocalized ciliary FFAR4 and PTGER4 and impaired regulated glucagon or insulin secretion, without affecting ciliary structure. Our findings provide index evidence that regulated hormone secretion by islet α and β cells is controlled by ciliary GPCRs providing new targets for diabetes.

Type 2 diabetes mellitus (T2D) is a pandemic disease affecting over 400 million patients worldwide (Carracher et al. 2018). Hallmarks of T2D include elevated blood glucose levels, inadequate circulating insulin, and excessive glucagon. Although glucose is a primary mediator of insulin and glucagon release from pancreatic islets, circulating factors including free fatty acids, amino acids, neurotransmitters, and hormones like incretins can play critical roles (Moullé et al. 2017). Accordingly, there is considerable interest in drugs that regulate insulin and glucagon secretion, notably drugs that regulate the G protein-coupled receptors (GPCRs) for the incretins glucagon-like peptide 1 (GLP-1) and glucose-dependent insulinotropic peptide (GIP) (Bailey 2020). Hormone-sensing GPCRs contribute to many aspects of α- and β-cell function, including regulated insulin and glucagon secretion (Moullé et al. 2017; Riddy et al. 2018). Recent studies suggest that primary cilia play critical roles in the β cells of the pancreatic islet (Volta et al. 2019; Hughes et al. 2020), but the molecular nature of that function is unclear. Here, we identify specific GPCRs that localize to islet α- and β-cell cilia and regulate glucagon and insulin secretion.

The primary cilium is a membrane- and microtubule-based sensory organelle protruding from the apical cell surface and is highly enriched with specialized GPCRs (Hilgendorf et al. 2016). Transport of GPCRs into the cilium is regulated by two major protein complexes, called the BBSome and the TULP3-IFT-A complex (Badgandi et al. 2017), both discovered in this laboratory (Nachury et al. 2007; Mukhopadhyay et al. 2010). The BBSome, named for Bardet-Biedl syndrome, is an eight-protein stoichiometric complex that critically regulates the dynamic trafficking of GPCRs in and out of cilia, notably by controlling ciliary exit. The TULP3-intraflagellar transport complex A (TULP3-IFT-A) complex regulates a key step in ciliary entry and is strongly required for ciliary signaling. Both pathways are coupled to a highly dynamic intraflagellar

transport pathway using kinesin and dynein motors and the conserved intraflagellar transport complexes IFT-B and IFT-A, which drives both ciliary assembly and signaling. Neither the BBSome nor TULP3 pathway is required for ciliary assembly.

Defects in primary cilia result in disorders, collectively called "ciliopathies," often present with metabolic syndromes including early onset obesity and eventual diabetes (Hilgendorf et al. 2016). Although most dramatically seen in syndromic ciliopathies, complex genetic and environmentally-induced defects in cilia may contribute broadly to metabolic disease.

Cilia are present on mouse and human islet α and β cells (Cano et al. 2004), and recent evidence has linked diabetic progression in ciliopathy patients to impaired insulin secretion (Pietrzak-Nowacka et al. 2010; Hearn 2019; Nesmith et al. 2019). Recent data also showed that dysregulation of cilia associated genes are linked to increased risk of T1D and T2D (Censin et al. 2017; Grarup et al. 2018; Kluth et al. 2019). Two rodent models have also correlated fewer ciliated α and β cells with impaired glucose-regulated insulin secretion (Östenson and Efendic 2007; Gerdes et al. 2014; Kluth et al. 2019). Moreover, β-cell-specific mouse knockouts (KOs) of the *Ift88* core ciliary gene and *Bbs4* component of the BBSome, critical for ciliary trafficking and signaling (Zimmerman and Yoder 2015; Kluth et al. 2019; Volta et al. 2019; Hughes et al. 2020), also show impaired glucose-stimulated insulin secretion (GSIS). These data argue that cilia are important in metabolic homeostasis and controlling the development of diabetes, raising the possibility that ciliary signaling through factors like GPCRs could regulate α- and β-cell function. However, the identity of GPCRs or other signaling regulators that localize to primary cilia and regulate β-cell and α-cell secretion have not been reported.

Here, we screened ciliary GPCRs as candidate regulators of insulin or glucagon output by islets. We discovered that GPCRs including FFAR4 and PTGER4, whose natural ligands include omega-3 free fatty acids like DHA and the prostaglandin PGE$_2$, localize to native α- and β-cell cilia and regulate insulin and glucagon secretion in response to pharmacological agonists through localized ciliary cyclic AMP (cAMP) signaling. We further found that agonists of receptors for omega-3 fatty acids can enhance glucose secretion in response to GLP1R agonists, indicating the potential for combination therapies for T2D.

Results

Identification of ciliary GPCRs regulating insulin and glucagon secretion

We hypothesized that α- and β-cell ciliary GPCRs transduce signals to regulate islet insulin or glucagon secretion and sought to identify GPCRs that localized to α- and β-cell cilia. From human pancreas transcriptome studies (Arda et al. 2016), we identified 96 GPCRs enriched in α and β cells compared to pancreatic duct cells (Fig. 1A). To assess ciliary localization, we expressed each candidate GPCR as a C-terminal GFP fusion protein and assessed subcellular

localization in the mouse pancreatic α-cell line α-TC9 (Powers et al. 1990) and in the mouse β-cell line MIN6 (Ishihara et al. 1993). Both cell lines are uniformly ciliated (>85%) at low or high density (Fig. 1B). We found that FFAR4, PTGER4, ADRB2, KISS1R, and P2RY14 localized to cilia in both MIN6 and α-TC9 cells (Supplemental Fig. S1A,B). To confirm ciliary localization of candidate GPCRs in native islet cells, we used validated antibodies that recognize the endogenous GPCR proteins (Hilgendorf et al. 2019) and found that endogenous free fatty acid receptor 4 (FFAR4) and prostaglandin E receptor 4 (PTGER4) localized to the primary cilium of MIN6 and α-TC9 cells. In contrast, endogenous KISS1R, a receptor for the peptide hormone kisspeptin, was not found localized to cilia in MIN6 and α-TC9 cells. Likewise, endogenous FFAR1, a functional homolog of FFAR4 that also binds omega-3 fatty acids, was not ciliary (Fig. 1C–H; Supplemental Fig. S1C, D). Thus, we successfully identified a selective set of GPCRs that localize to cilia in islet α- and β-cell lines.

Ciliary GPCRs regulate insulin and glucagon secretion

To test whether FFAR4 or PTGER4 regulate insulin or glucagon secretion, we exposed MIN6 or α-TC9 cells to selective agonists of these GPCRs and measured glucose-stimulated insulin secretion and glucose-stimulated glucagon secretion (GSGS) assaying at 1 h after treatment. MIN6 cells displayed glucose-dependent insulin secretion, and α-TC9 cells showed glucose-dependent glucagon secretion, as previously reported (Fig. 2A,B; Powers et al. 1990; Ishihara et al. 1993). We examined the effect of agonists for FFAR4 or PTGER4 on insulin or glucagon secretion. Both FFAR4 and PTGER4 agonist treatment augmented insulin secretion in a dose-dependent manner at elevated (16.7 and 25 mM) glucose concentrations (Fig. 2C,D). These higher glucose concentrations mimic postprandial glucose levels, compared to controls and are the basis of quantifying GSIS. Similarly, the FFAR4 agonist enhanced glucagon secretion at low (1 mM) glucose concentrations in α-TC9 cells (Fig. 2E), which is characteristic of agonist signaling for GSGS in α cells. A PTGER4 agonist did not potentiate GSGS in α-TC9 cells (Fig. 2F). We found that several agonists of GPCRs not localized to cilia in MIN6 or α-TC9 cells also potentiated glucose-regulated insulin or glucagon secretion. This included exposure to agonists for KISS1-R (Supplemental Fig. S2A,B) and to TUG424, a selective FFAR1 agonist (Supplemental Fig. S2F). In contrast to these results, we observed no detectable effect on MIN6 insulin secretion or α-TC9 glucagon secretion following similar exposure to agonists of ADRB2 or P2RY14 (Supplemental Fig. S2C,D). Together, these data indicate that FFAR4 and PTGER4 are ciliary GPCRs that can potentiate glucose-regulated insulin and glucagon secretion. Glucagon-like peptide 1 receptor (GLP1R) is a GPCR critical for GSIS but is not known to localize to islet cilia. GLP1R agonists comprise an important standard treatment for type 2 diabetes (Gentilella et al. 2019). We observed that stimulation of GSIS by the GLP1R agonist Exendin-4 showed a similar magnitude of effect to FFAR4 agonists (Supplemental Fig. S2E). This
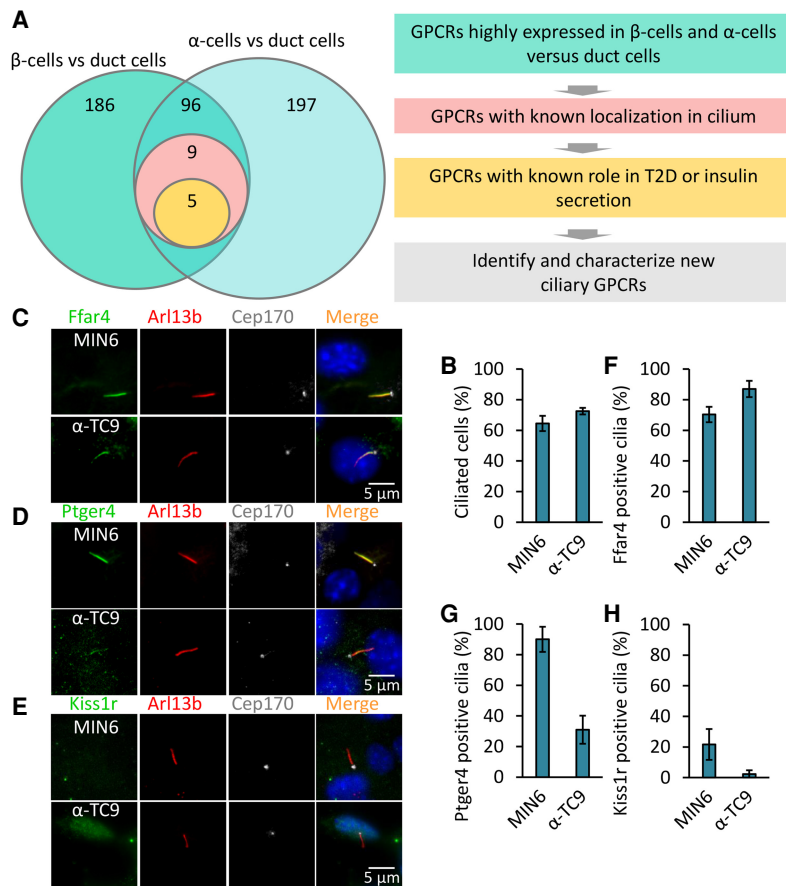
Figure 1. Identification of ciliary GPCRs regulating insulin and glucagon secretion. (*A*) Schematic of the screen to identify ciliary GPCR in human pancreatic α and β cells. Candidate GPCRs were selected based on known localization in the cilium and for links to T2D or insulin/glucagon secretion. (*B*) MIN6 and α-TC9 cells are ciliated. MIN6 and α-TC9 cells were grown to confluence. Ciliated cells were examined by confocal fluorescence microscopy using acetylated tubulin and Arl13b antibodies, and quantified. (*C–H*) Endogenous Ffar4 and Ptger4 but not Kiss1r localize to the primary cilium of MIN6 and α-TC9 cells. MIN6 and α-TC9 cells grown to confluence were immunostained with the indicated antibodies (*C–E*). Percentages of GPCRs-positive ciliated cells (labeled Ar13b) are shown in *F–H*. Error bars in *B* and *F–H* represent mean ± SD. $n = 3$ independent experiments with 100–300 cells scored per experiment.

suggests that FFAR4 agonists may show therapeutic effects of similar magnitude to GLP1R agonists as monotherapies. To evaluate whether GLP1R potentiation of glucose-dependent insulin secretion can be enhanced in combination with FFAR4 activation, we simultaneously stimulated GLP1R with the agonist Exendin-4 and FFAR4 with TUG891 in MIN6 cells. Compared to exposure to Exendin-4 or TUG891 alone, glucose-dependent insulin secretion by MIN6 cells was substantially increased by simultaneous Exendin-4 and TUG891 (Supplemental Fig. S2E). We observed a similar effect with combined exposure to TUG424, a FFAR1 agonist, and TUG891 (Supplemental Fig. S2F). Thus, FFAR4 agonists could potentially combine with GLP1R and FFAR1 agonists, suggesting these receptors signal via distinct but cooperating signaling pathways.

TULP3 is required for trafficking FFAR4 and PTGER4 to islet cell cilia

TULP3 is a crucial regulator of GPCR trafficking and localization to cilia and is thought to work primarily by controlling receptor entry into cilia. Relevant to these studies, depletion of TULP3 impairs localization of FFAR4 to the cilium of 3T3-L1 preadipocytes and attenuates FFAR4 agonist-regulated adipogenesis (Hilgendorf et al. 2019). However, prior studies have not assessed the requirement for TULP3 in GPCR trafficking in islet cell

cilia (Badgandi et al. 2017). To test this possibility, we used CRISPR-Cas9 to generate MIN6 and α-TC9 cells lacking TULP3 (Fig. 3A,B). Consistent with prior work in other cells, deletion of TULP3 from primary cilia in MIN6 and α-TC9 cells did not detectably affect ciliation (Fig. 3C,D). However, TULP3 deletion in these cells reduced localization of the ciliary signaling protein ARL13B to unmeasurable levels, consistent with reports in other cell types (Supplemental Fig. S3A,B; Legué and Liem 2019). Moreover, we found that deletion of TULP3 strongly decreased localization of FFAR4 and PTGER4 to cilia in MIN6 and α-TC9 cells (Fig. 3E–G) but did not affect the mRNA or protein expression level of *FFAR4* and *PTGER4* (Supplemental Fig. S3E,F). In addition, this decrease of FFAR4- or PTGER4-regulated GSIS or GSGS was rescued by expression of human TULP3, confirming the specificity of the effect (Supplemental Fig. S3G–J). Thus, localization of FFAR4 and PTGER4 to cilia in islet cells is TULP3-dependent.

FFAR4- and PTGER4-regulated insulin or glucagon secretion is cilia-dependent

To test whether islet α and β cells require ciliary trafficking of FFAR4 and PTGER4 to transduce metabolic cues and potentiate insulin and glucagon secretion, we treated MIN6 or α-TC9 cells lacking TULP3 with the specific
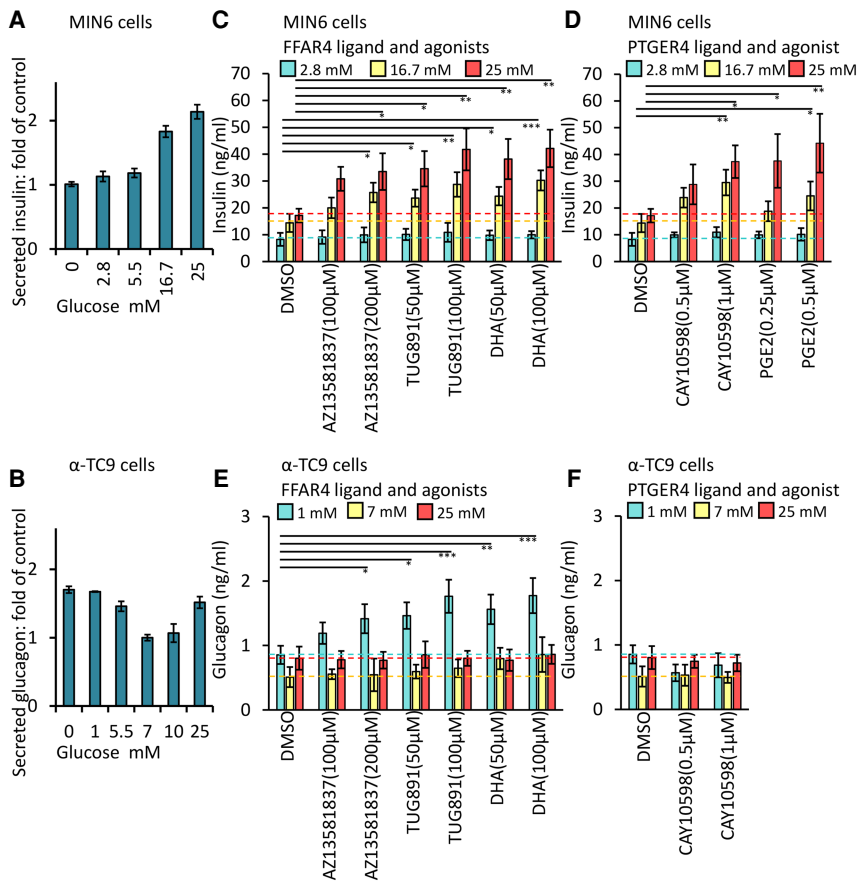
Wu et al.

Figure 2. Ciliary GPCRs agonists promote GSIS and GSGS. MIN6 (*A*) and α-TC9 (*B*) cells responded in a dose-dependent manner to glucose. GSIS (*C,D*) and GSGS (*E,F*) induced by elevation (from 2.8 to 25 mM) or decrease (from 25 to 1 mM) of glucose levels for 1 h and then effects of agonists on insulin or glucagon secretion were evaluated. (*A–F*) Equal numbers of MIN6 or α-TC9 cells were plated onto 96-well plates (1×10^5/well) for overnight culture before the secretion assay. Error bars represent mean ± SD. $n = 3$ independent experiments. One-way ANOVA: (*) $P < 0.05$, (**) $P < 0.01$, (***) $P < 0.001$.

FFAR4 and PTGER4 agonists and examined effects on insulin and glucagon secretion. If FFAR4 or PTGER4 regulates insulin or glucagon secretion in a cilia-dependent manner, agonist or ligand treatment should enhance glucose-stimulated insulin or glucagon secretion in control cells but not in cells lacking TULP3. Insulin or glucagon content were not significantly altered in MIN6 or α-TC9 cells lacking TULP3 (Fig. 3H,I), supporting that TULP3 depletion did not affect hormone production or accumulation. TULP3 loss also did not affect basal levels of glucose-stimulated insulin or glucagon secretion of MIN6 and α-TC9 cells (Fig. 3J,K). Central to our hypothesis, loss of TULP3 impaired the potentiation by FFAR4 or PTGER4 agonists of glucose-dependent insulin secretion by MIN6 cells (Fig. 3L; Supplemental Fig. S3C) and glucagon secretion by α-TC9 cells (Fig. 3M) but did not affect FFAR4 or PTGER4 expression levels by qPCR (Supplemental Fig. S3E), nor did it affect FFAR4 or PTGER4 protein levels, arguing that ciliary localization is critical for FFAR4 and PTGER4 to enhance signaling in islet cells. Importantly, the decrease of insulin and glucagon secretion following Tulp3 deletion was rescued by expression of human TULP3, confirming the specificity of the effect (Supplemental Fig. S3F–I). In contrast, deletion of TULP3 did not reduce potentiation of insulin or glucagon secretion by TUG424, an agonist for FFAR1, which is not localized to cilia (Fig. 3L,M). Likewise, TULP3 knockout did not affect KISS1R-regulated insulin or glucagon secretion (Sup-

plemental Fig. S3C,D). Thus, our work provides evidence that FFAR4 or PTGER4 agonists selectively promote insulin or glucagon secretion via TULP3-dependent localization mechanisms in primary cilia of MIN6 or α-TC9 cells.

Localization of FFAR4 and PTGER4 to cilia in primary human and mouse islet cells

Previous studies have shown that human and murine islet cells are ciliated (Green 1980; Cano et al. 2004). To confirm and extend these observations, we first quantified ciliation of islet α, β, and δ cells from mice or human fresh cadaveric donors and found that both mouse and human endocrine cells are efficiently ciliated, to ~62%, 70%, and 75% in mouse islets and to ~32%, 41%, and 33% in human α, β, and δ cells (Fig. 4A,B). We suspect that these numbers are a minimum estimate of the number of ciliated islet cells in vivo because of modest loss of viability or ciliation upon isolation of islets, especially the human patient samples. Supporting our findings with α- and β-cell lines, we found that FFAR4 localized to the primary cilium of pancreatic α and β cells in mouse and human islets and that this ciliary localization persisted even after dissociation and flow cytometry-based purification of α and β cells from isolated islets (Fig. 4C–F; Supplemental Fig. S4A,B). The specificity of the anti-Ffar4 antibody in human cells was validated through peptide blocking assays (Supplemental Fig. S4I) and previously validated for the highly
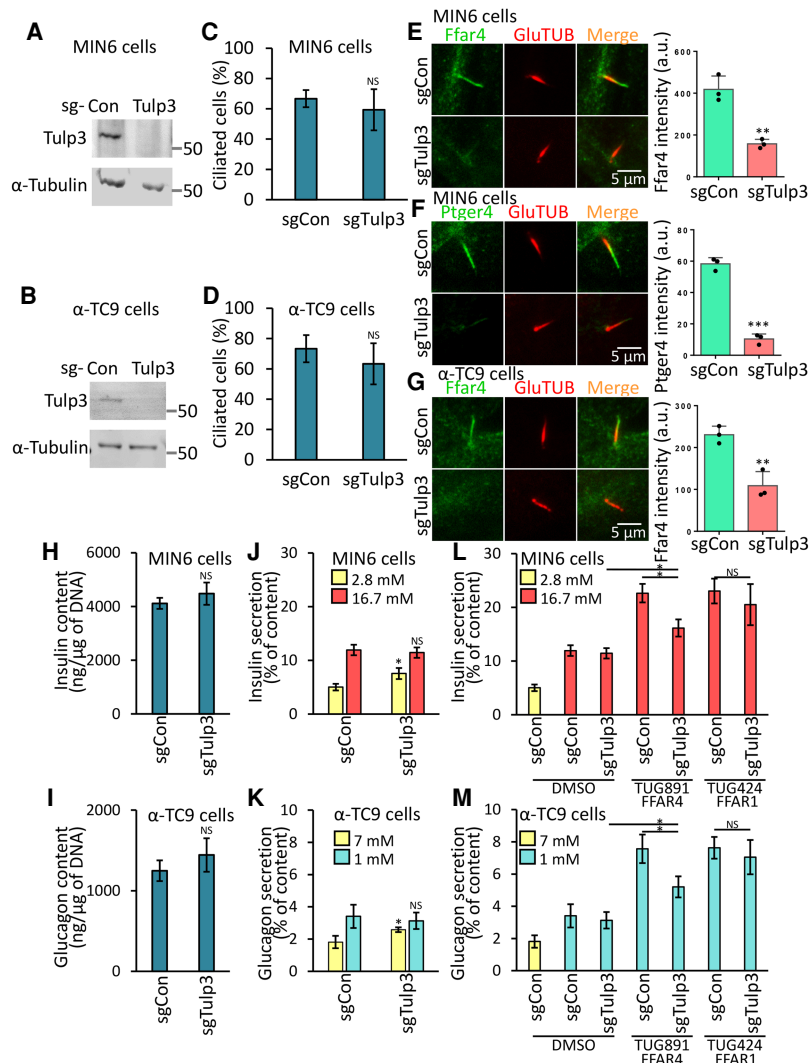
Figure 3. Ffar4-regulated GSIS and GSGS are Tulp3-dependent in pancreatic α- and β-cell lines. (*A–D*) Loss of Tulp3 does not affect cilia formation in MIN6 and α-TC9 cells. Immunoblot showing depletion of TULP3 in MIN6 (*A*) and α-TC9 (*B*) sgTulp3 cell line. Control MIN6 (*C*) and α-TC9 (*D*) cells (sgCon) and Tulp3 knockout cell lines (sgTulp3) grown to confluence. Ciliated cells were examined by confocal fluorescence microscopy using acetylated tubulin antibody, and quantified. (*E–G*) Loss of Tulp3 prevents ciliary GPCRs trafficking in MIN6 and α-TC9 cells. Control MIN6 (*E,F*) and α-TC9 (*G*) cells and Tulp3 knockout cell lines grown to confluence were immunostained with indicated antibodies. (*E–G, right*) The graph shows the fluorescent intensity of the indicated GPCR proteins that colocalize with the cilium. *n* = 3 independent experiments with 50∼100 cilia scored per experiment. (*H,I*) Insulin and glucagon content was unchanged in Tulp3 knockout versus control MIN6 (*H*) or α-TC9 (*I*) cells. The cells were incubated with 2.8 mM (MIN6) and 7 mM (α-TC9) glucose buffer for 1 h prior to collection. (*J–M*) GSIS (*J,L*) and GSGS (*K,M*) induced by elevation (from 2.8 to 16.7 mM) or decrease (from 7 to 1 mM) of glucose levels for 1 h and then effects of agonists on insulin or glucagon secretion were evaluated. (*J,K*) GSIS and GSGS were unchanged in Tulp3 knockout versus control MIN6 (*J*) or α-TC9 (*K*) cells. (*L,M*) Ffar4-regulated GSIS (*L*) and GSGS (*M*) are cilia-dependent. (*J–M*) Equal numbers of MIN6 or α-TC9 cells were plated onto 96-well plates (1 × 10^5/well) for overnight culture before the secretion assay. Error bars in *C–M* represent mean ± SD. *n* = 3 independent experiments. Two-tailed unpaired Student's *t*-test: (*) *P* < 0.05, (**) *P* < 0.01, (***) *P* < 0.001, (NS) nonsignificant.

conserved mouse FFAR4 epitope in mouse knockouts (Hilgendorf et al. 2019). PTGER4 also localized to the primary cilium in β cells; however, compared to FFAR4, the degree of PTGER4 localization to α-cell cilia was minimal (Fig. 4G–J; Supplemental Fig. S4C,D). We next examined the effects of FFAR4, PTGER4, and KISS1R agonists on insulin or glucagon secretion from mouse or human islets. Addition of agonists promoted insulin or glucagon secretion in mouse or human islets (Supplemental Fig. S4E–H). Consistent with our cell line data, the PTGER4 agonist did not affect glucagon secretion (Supplemental Fig. S4F,H). Taken together, our data show that FFAR4 and PTGER4 localize to the cilium in mouse and human endocrine cells and regulate insulin and glucagon secretion.

FFAR4- and PTGER4-regulated islet hormone secretion is cilia-dependent

To test whether FFAR4- and PTGER4-regulated hormone secretion in primary pancreatic islets requires TULP3, we infected dispersed primary human islet cells with lentivirus expressing shRNA to knock down *TULP3*, reaggregated these cells into pseudoislets (Peiris et al. 2018), and measured glucose-dependent insulin or glucagon secretion. Lentiviral GFP coexpression permitted sorting and isolation of virus-infected cells. Greater than 50% knockdown of *TULP3* mRNA was demonstrated by qRT-PCR (Supplemental Fig. S5A,B). Total insulin or glucagon content was not significantly altered after *TULP3* knockdown (Supplemental Fig. S5C–F). Similar to our islet cell line studies, depletion of *TULP3* mRNA did not affect insulin or glucagon secretion in response to glucose changes alone (Fig. 5A,C,E,G; Supplemental Fig. S5G,M,J,P) but did significantly attenuate FFAR4 and PTGER4 agonist-regulated insulin or glucagon secretion (Fig. 5B,D,F,H; Supplemental Fig. S5H,N,I,O,K,Q). Similar to our cell line studies, exposure to selective FFAR1 and KISS1R agonists (whose receptors do not localize to islet cilia) also stimulated insulin or glucagon secretion, and this effect was not altered by *TULP3* islet knockdown (Fig. 5B,D,F, H; Supplemental Fig. S5H,I,K,L,N,O,Q,R). Thus, our findings establish that FFAR4- and PTGER4-regulated insulin
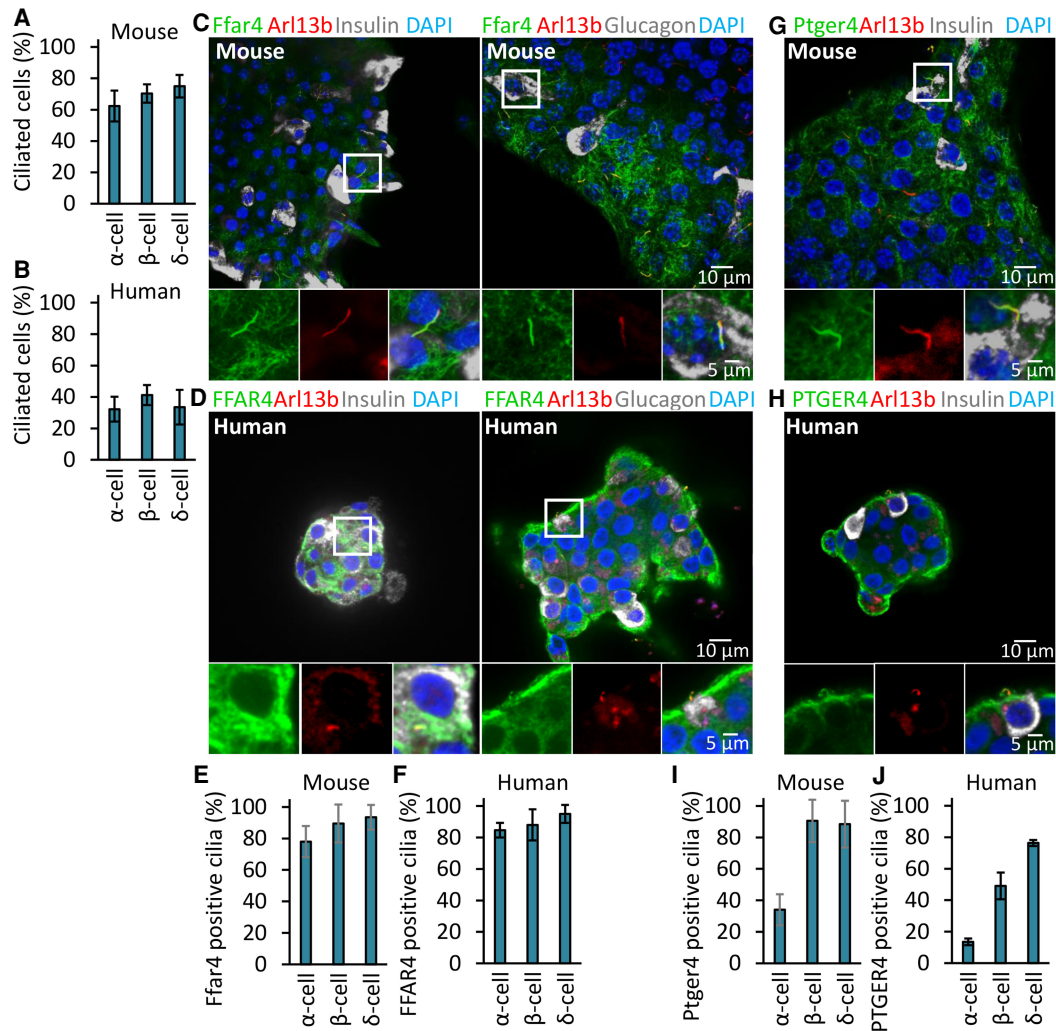
Wu et al.

Figure 4. FFAR4 and PTGER4 are a ciliary GPCR displayed by mouse and human pancreatic α and β cells. (A,B) α, β, and δ cells are ciliated in mouse (A) and human (B) islets. Ciliated cells were examined by confocal fluorescence microscopy using acetylated tubulin, Arl13b, insulin, glucagon, and somatostatin antibodies, and quantified. (C–J) Endogenous Ffar4 and Ptger4 localize to the primary cilium of α and β cells in mouse (C,G,E,I) and human (D,H,F,J) pancreatic islet. (E,F,I,J) Percentages of GPCRs-positive mouse (E,I) and human (F, J) ciliated α, β, and δ cells (labeled Ar13b) are shown. Error bars in A,B,E,F,I,J represent mean ± SD. $n = 3$ independent experiments with 100–300 cells scored per experiment.

or glucagon secretion by primary islet cells are TULP3-dependent and function efficiently in mouse and human islets.

FFAR4 signaling raises ciliary cAMP to promote insulin or glucagon secretion

To identify molecular signaling mechanisms underlying FFAR4 or PTGER4 potentiation of insulin or glucagon secretion, we investigated ciliary cAMP signaling, which we established in our recent study showing that omega-3 fatty acids activate ciliary FFAR4 cAMP signaling and stimulate adipogenesis (Hilgendorf et al. 2019). Adenylyl cyclases (ACs) catalyze the conversion of adenine triphosphate (ATP) into cAMP in response to a wide range of extracellular signals. In mammals, there are nine

membrane-associated ACs. The calcium-regulated type 3 adenylyl cyclase (AC3), an established cilia marker, is highly and predominantly expressed in primary cilia in different tissues, including pancreas, adipose tissue, kidney, and brain (Qiu et al. 2016). Moreover, recent human genetics studies show that mutation of the *ADCY3* gene encoding AC3 is among those genes most clearly associated with T1D and T2D (Censin et al. 2017; Grarup et al. 2018). We observed that AC3 selectively localizes to cilia in MIN6 and α-TC9 cells (Supplemental Fig. S6A), supporting the idea that specific ACs can localize to cilia in islet cells. To test the hypothesis that FFAR4 activation promotes insulin or glucagon secretion by modulating ciliary cAMP, we transduced MIN6 and α-TC9 cells with a ciliary targeted cAMP sensor optimized for live cell imaging (cilia cADDIS) (Moore et al. 2016; Jiang et al. 2019).
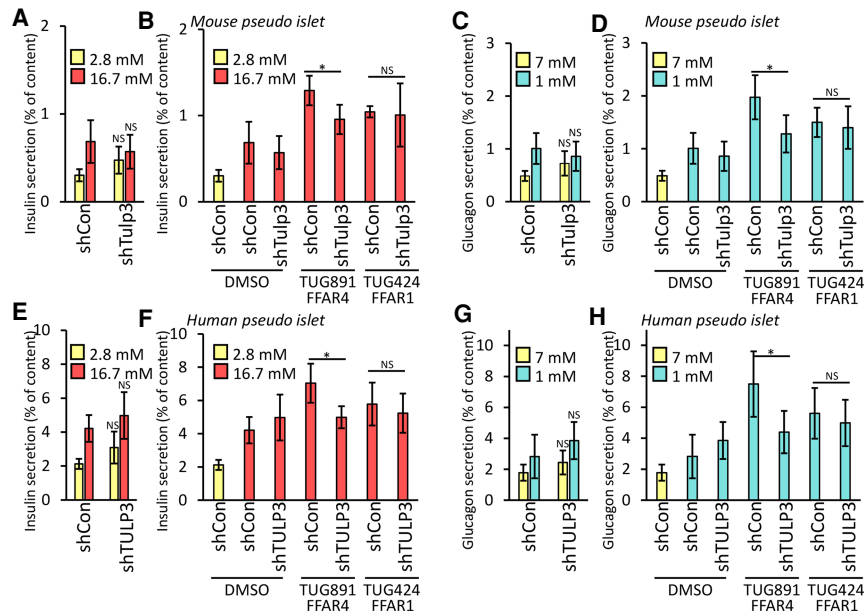
Figure 5. FFAR4-regulated GSIS and GSGS are cilia-dependent in pancreatic islet. GSIS (*A*,*E*) and GSGS (*C*,*G*) was unchanged in Tulp3 knockdown (shTulp3) versus scrambled control (shCon) mouse (*A*,*C*) or human (*E*,*G*) pseudoislets. (*B*,*D*,*F*,*H*) Ffar4-regulated GSIS (*B*,*F*) and GSGS (*D*,*H*) are cilia-dependent in mouse (*B*,*D*) and human (*F*,*H*) pseudoislets. GSIS (*A*,*B*,*E*,*F*) and GSGS (*C*,*D*,*G*,*H*) induced either by increasing (from 2.8 to 25 mM) or decreasing (from 25 to 1 mM) glucose levels for 1 h and effects of agonists on insulin or glucagon secretion were evaluated. Error bars in *A*–*H* represent mean ± SD. $n = 4$ independent experiments. Two-tailed unpaired Student's *t*-test: (*) $P < 0.05$, (NS) nonsignificant.

This cAMP sensor responds to a proximal increase in cAMP levels by decreasing green fluorescence signal intensity. Within 120 sec of MIN6 or α-TC9 exposure to the FFAR4 agonist TUG891, we observed progressively increased ciliary cAMP levels (Fig. 6A,B; Supplemental Fig. S6B). As a control, a selective FFAR1 agonist did not potentiate ciliary cAMP levels, despite activating GSIS, supporting that FFAR1 works via a distinct, nonciliary pathway. cAMP may activate at least two downstream cAMP effector pathways, the cAMP-dependent protein kinase A (PKA) or by the cAMP-regulated small GTPase nucleotide exchange factor, EPAC. Pharmacological inhibition of EPAC prevented FFAR4 agonist-stimulation of both insulin and glucagon secretion (Fig. 6C,D). Inhibition of PKA also inhibited FFAR4 agonist-stimulated insulin secretion but not glucagon secretion (Fig. 6E,F). Thus, FFAR4 signaling likely potentiates insulin secretion by activating localized ciliary cAMP signaling via both EPAC and PKA activity. Interestingly, prior studies show that FFAR4 agonist regulated adipogenesis through activation of localized ciliary cAMP and EPAC but not detectably via PKA (Hilgendorf et al. 2019). Examining potentiation of secretion by PTGER4, we found that inhibition of EPAC, but not PKA, prevented PTGER4 agonist-enhanced insulin secretion (Fig. 6C,E). We do not currently understand the observed differences between FFAR4 and PTGER4 signaling for activating PKA, but there may be distinct mechanisms and signaling thresholds that underlie the different requirements. Together, these studies identify cAMP-dependent mechanisms of ciliary GPCR signaling, executed through overlapping but distinct pathways.

Discussion

Pancreatic islet cells are vital regulators of metabolism that integrate diverse, dynamic signals to optimize their output of insulin and glucagon. Although glucose is a primary regulator of insulin and glucagon secretion by islets, other important signals responding to metabolic flux or feeding state are recognized as crucial controllers of islet hormone output. Together, multiple signals from (1) gut-derived responses to dietary sources, (2) the autonomic and central nervous system, and (3) peripheral organs like fat, liver, and other islet cell subtypes can be integrated to regulate islet cell hormone output and match dynamic physiological demands (Campbell and Drucker 2015; Ribeiro et al. 2018). Intensive investigations have focused on identifying the cellular and molecular signaling elements in islets that integrate and orchestrate islet hormone output (Noguchi and Huising 2019). Work here provides index evidence that islet cell primary cilia are organizers of signaling by specific G-protein-coupled receptors that respond to native ligands and synthetic agonists to regulate islet insulin and glucagon secretion. Findings here also delineate specific intracellular responses to ciliary GPCR activation, via cAMP, and suggest how ciliary signaling logic could integrate multiple cues to optimize hormonal output and metabolic control.

Our work reveals multiple ciliary GPCRs as conserved regulators of insulin and glucagon output by mouse and human islets. Depletion of TULP3, a regulator of GPCR trafficking to cilia in pancreatic α- and β cells, provided critical evidence that ciliary localization of GPCRs like FFAR4 and PTGER4 is required for potentiation of glucose-stimulated insulin or glucagon secretion by specific agonists in vitro and in ex vivo islet cultures. Agonist activation of ciliary FFAR4 resulted in a rapid increase in cAMP levels. The importance of cAMP signaling downstream of FFAR4 and PTGER4 in MIN6 was supported by the ability of inhibitors of the cAMP effectors EPAC, a guanine-nucleotide exchange factor, and protein kinase A to block insulin or glucagon secretion. The demonstration that these signaling effects are observed in α- and β-
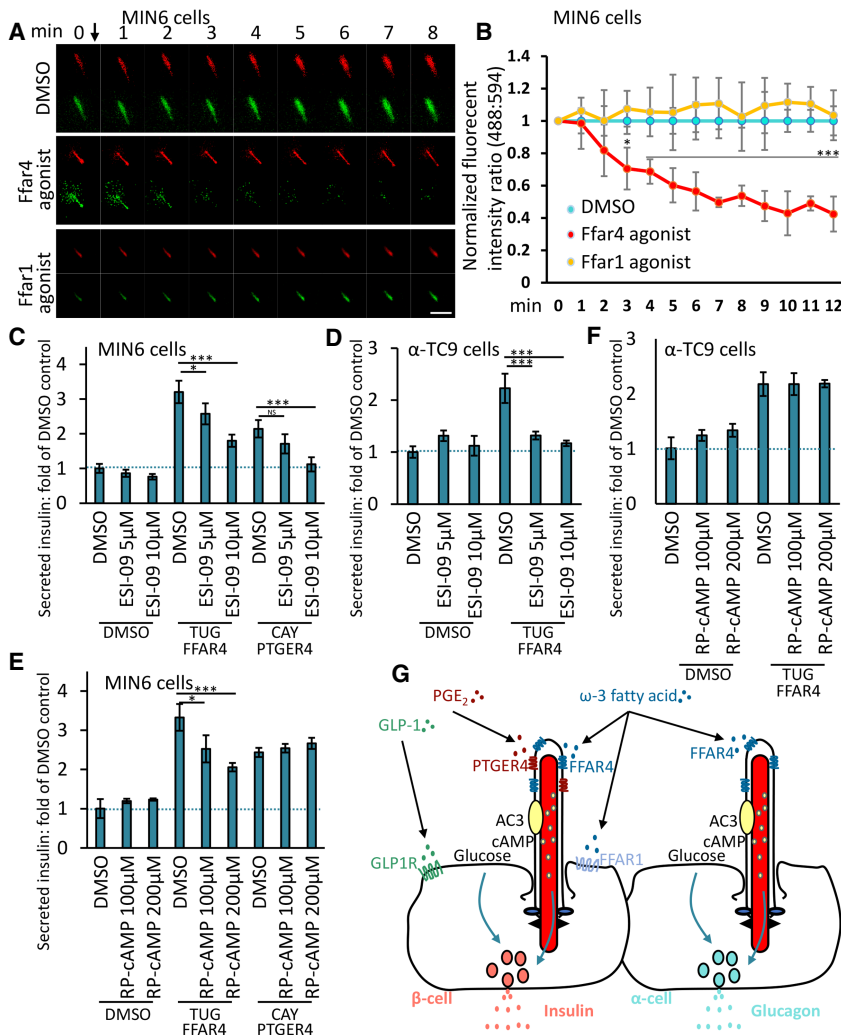
Wu et al.

Figure 6. FFAR4 regulates GSIS and GSGS via cAMP. (*A*) Representative images showing the cADDIS cAMP sensor (green) and cilia (red) offset in MIN6 cells. Scale bar, 2 μm. (*B*) Background subtracted ratio of fluorescence intensities are normalized to DMSO control and 0-sec time point. $n = 3$ for FFAR4 agonist and DMSO control ± SD, where n is the average of all cilia measured per well. (*C–F*) Inhibition of EPAC attenuates Ffar4-regulated GSIS and GSGS in a dose-dependent manner. MIN6 (*C,E*) and α-TC9 (*D, F*) cells were stimulated with GPCR agonists in the presence of an inhibitor of EPAC (ESI-09) or PKA (Rp-cAMPS) for the first 1 h. Error bars in *C–F* represent mean ± SD. $n = 3$ independent experiments. One-way ANOVA: (*) $P < 0.05$, (***) $P < 0.001$, (NS) nonsignificant. (*G*) Model for ciliary GPCR-regulated insulin or glucagon secretion. FFAR4 localized to the cilia in α and β cell is activated by ω-3 fatty acids to promote glucose-stimulated insulin or glucagon secretion. PTGER4 localized to cilia in β cells is activated by PGE2 to regulate glucose-stimulated insulin secretion. GLP1R and FFAR1 localized to the plasma membrane are activated by GLP-1 or ω-3 fatty acid to regulate insulin secretion, which can cooperate with FFAR4-stimulated insulin secretion.

cell lines argues that TULP3-dependent ciliary GPCR signals are cell-autonomous (Fig. 6G).

The demonstration here that ciliary FFAR4 directly regulates insulin secretion in β cells parallels our observations in preadipocytes, where FFAR4 agonists can stimulate both preadipocyte mitogenesis and differentiation to adipocytes (Hilgendorf et al. 2019). We also observed there that cilia are strongly required for adipocyte differentiation, of which the ω-3 fatty acid/FFAR4 pathway is a central contributor. As another key factor in adipogenesis is insulin signaling, we now consider how a combination of ω-3 fatty acids and glucose during feeding would cooperate to stimulate insulin secretion, then allowing ω-3 fatty acids and insulin to cooperate to induce de novo adipogenesis. The potential of ω-3 fatty acids to prolong insulin levels and what perduring levels of ω-3 fatty acids and insulin would be sufficient to initiate adipogenesis is a remaining question.

We additionally show that ciliary FFAR4 regulates glucagon secretion by α cells. Specifically, in vivo and ex vivo, loss of ciliary FFAR4 in α and β cells impairs FFAR4 agonist-regulated insulin and glucagon secretion. We found that this process is also strongly linked to ciliary pro-

duction of cAMP (Fig. 6G). Although cAMP is generally considered as an amplifier of insulin secretion, which is more directly triggered by Ca^{2+} elevation in the β cells (Shibasaki et al. 2004), it was not previously reported that subcellular organelle signaling, like in islet cell cilia, might underlie this effect. cAMP is synthesized by adenylyl cyclases. In mammals, there are nine membrane-associated ACs. Here, we found that AC3 localizes to the cilia in MIN6 and α-TC9 cells. This suggests that ciliary AC3 may be activated by FFAR4 and then increase the cAMP level in the cilium. However, we recognize other ACs like AC5/6 may also be involved; recent data showed that mutation of *ADCY3*, *ADCY5*, and *ADCY6* are each strongly associated with T1/T2D (Hodson et al. 2014; Censin et al. 2017; Grarup et al. 2018). We hypothesize that specific cAMP effectors may work locally at cilia or centrioles to control signaling or transport processes. In many organisms including unicellular protists, flagella, precursors of primary cilia, are localized next to zones of organized endocytosis and exocytosis. The specific configuration of cilia in the context of islet cells is therefore of interest, and future studies could address how localized cAMP signals are

propagated to the secretory vesicles in active zones of islet cells. In addition to signaling mechanisms revealed here, prior reports (Sundström et al. 2017) suggest that FFAR4 stimulation may lead to activation of phospholipase C (PLC) and subsequent elevation of intracellular Ca^2; we have found that exposure of MIN6 and α-TC9 cells to PLC inhibitor U73122 also attenuates FFAR4-stimulated insulin and glucagon secretion (data not shown). Additional studies may inform how the specific ciliary GPCRs locally transmodulate multiple signaling pathways and whether this multiplexed signaling can be achieved by dynamic control of signaling within the cilium.

PGE$_2$ production is activated in response to various forms of pancreatic damage and is expected to work via four independent receptors PTGER1–4, often called EP1–4. Of these four, only PTGER4/EP4 is ciliary (Jin et al. 2014; PK Jackson, CT Wu, KI Hilgendorf, et al., unpubl.) and is the major form linked to Gα_s and cAMP production. Prior studies have shown a protective role for EP4 on β-cell survival and proliferation (Carboneau et al. 2017a), but EP3 may have opposing effects. The presence of inflammatory receptors like PGTER4 may couple localized pancreatic or more global inflammatory responses to islet output of insulin. Systemic delivery of high levels of PGE$_2$ appear to lower insulin secretion (Robertson 1988; Carboneau et al. 2017b), but the selective effects of PGE$_2$ on β-cell proliferation or survival versus direct effects on insulin secretion or other effects of PGE$_2$ outside the β cell are not well separated. The broader context of activating PGE$_2$ levels in pancreatic islets may cause a variety of effects. Here, by using selective PTGER4 agonists, we show that direct effects on cAMP, via its ciliary signaling channel, have a positive effect on insulin release. Previous studies have suggested that PGE2 may work through a different PGE2 receptor PTGER3 to inhibit insulin secretion, but a consensus view on PGE2 control of insulin secretion has not emerged (Carboneau et al. 2017b). Why precisely PGE2 signaling should increase insulin secretion and under which normal or pathophysiological contexts would PGE2 alter insulin secretion remain outstanding questions. Even less is known about PGE2 signaling and glucagon secretion, but we found that the EP4 expression level in the cilia is low or absent in α cells.

Our work also revealed evidence of additive or synergistic regulation of β-cell insulin secretion by a combination of FFAR4 and FFAR1 agonists or by FFAR4 and GLP1R agonist combinations (Supplemental Fig. S2E,F). This is supported by recent studies suggesting that FFAR1 and FFAR4 signaling cooperate to stimulate insulin secretion (Croze et al. 2020). Neither FFAR1 (Fig. 1) nor GLP1R (C-T Wu and PK Jackson, unpubl.) are observed to localize to cilia. Consistent with its localization, FFAR1-regulated insulin and glucagon secretion is TULP3-independent. Thus, outcomes here suggest that islet hormone secretion responds to activation of GPCRs in different subcellular compartments (Fig. 6G) as alternate or integrated signals. It has been reported that FFAR1 and FFAR4 bind to medium- to long-chain fatty acids, including ω-3 fatty acids like α-linolenic acid, eicosapentaenoic acid (EPA), and docosahexaenoic acid (DHA), leading to enhanced insulin and glucagon secretion (Ichimura et al. 2014). However, it is not entirely clear that FFAR1 and FFAR4 signaling results from precisely the same natural ligands, nor how typical dietary fluxes activate these individual receptors. Unlike FFAR4 agonists, FFAR1 agonists stimulate calcium influx, not cAMP (Croze et al. 2020). Synergy between cAMP and calcium signals appears common to various combinations of FFAR4, FFAR1, and GLP1R agonists (Supplemental Fig. S2E,F). GLP1R signaling appears to induce intracellular Ca^{2+} transients in addition to cAMP signaling (Meloni et al. 2013). In one model, ciliary FFAR4-cAMP signaling might activate docked, active zone vesicles, possibly through EPAC2-dependent activities at the secretory zone. This docking could augment or synergize with GLP1R- or FFAR1-dependent calcium influx to increase the efficiency or number of presecretory vesicles triggered for release near the active zone.

Based on the signaling we observed here in isolated islets, we can propose that the apical position of primary cilia in pancreatic islets provides a critical architecture that integrates islet cell crosstalk. This could represent both homotypic (β-cell to β-cell) and heterotypic (β-cell to α-cell) paracrine signals from nearby islet cells but also global endocrine and metabolite signals. We can imagine a range of signaling inputs, some commonly used and some more specialized, that would control insulin and glucagon secretion, and more broadly in other islet subtypes. There is the intriguing possibility that ciliary signaling in multiple islet cell types allows an integration of dietary and neuroendocrine signals, ensuring metabolic homeostasis and rapid responses to specialized conditions.

The integrated, multisystem approach used here to identify ciliary GPCRs and mechanisms that regulate human insulin and glucagon secretion can be readily expanded. Further studies could take advantage of the tools and approaches generated here, including development of Tulp3-deficient α- and β-cell lines, pseudoislet-based genetic methods for generating primary human islets lacking TULP3, and measures of agonist-dependent hormone secretion. For example, based on prior studies, dynamic physiological changes like sexual maturation or pregnancy (Koemeter-Cox et al. 2014), potentially via KISS1R, or inflammatory states like diabetes (Sarchielli et al. 2017), potentially via PGE2/PTGER4 signaling, could alter islet ciliary signaling. It would be especially interesting if age- or disease-dependent degeneration of ciliary signaling might underlie islet dysfunction and diabetes.

Materials and methods

Human islet procurement

Deidentified human pancreatic islets were obtained from organ donors without a history of glucose intolerance with <15 h of cold ischemia time. Islets were procured through the Integrated Islet Distribution Program, Alberta Diabetes Institute IsletCore, and the International Institute for the Advancement of Medicine.

Mouse islet isolation

Islets were isolated from male C57BL/6 mice at 2–4 mo of age using injection of collagenase P (Roche Diagnostics 11213865001)

Wu et al.

into the pancreatic duct, surgically removing the infused pancreas and placing it into 50-mL conical tubes containing 4 mL of HBSS/Ca/HEPES solution (1 L of Hanks balanced salt solution [HBSS], 2 mM $CaCl_2$, 20 mM HEPES). Mouse pancreata were incubated for 12 min in a 37°C water bath. The digested pancreata were than washed three times in ice-cold HBSS/Ca/HEPES solution. The pancreas tissue was disrupted by vigorous hand shaking of the tubes for 1 min at a rate of three shakes per second. The islets were isolated from acinar tissue on a Histopaque-1077 gradient (Sigma-Aldrich H8889). After three additional washes by RPMI 1640 (Gibco), islets were handpicked under a dissecting microscope and cultured in RPMI 1640, 2.25 g/dL glucose, 1% (v/v) penicillin/streptomycin (Gibco), and 10% fetal bovine serum (HyClone).

Human and mouse pseudoislet generation

Human or mouse islets were dissociated into a single-cell suspension by enzymatic digestion (Accumax, Invitrogen). For each experimental condition, ~1×10^6 cells were transduced with SMARTvector lentiviral shRNA particles targeting mouse Tulp3, human TULP3, or SMARTvector nontargeting control particles (Dharmacon Thermo Scientific) corresponding to 1×10^9 viral units in 1 mL as determined by the Lenti-X qRT-PCR titration kit (Clontech). Lentiviral-transduced islets cells were cultured in 96-well ultralow-attachment plates (Corning) and cultured for 3 d at 37°C in 5% CO_2. After 3 d, pseudoislets were transferred to six-well ultralow-attachment plates and cultured 2 d prior to further molecular or physiological analysis. The islets were cultured in the following culture medium: RPMI 1640 (Gibco), 2.25 g/dL glucose, 1% (v/v) penicillin/streptomycin (Gibco), and 10% fetal bovine serum (HyClone). Human TULP3 shRNA targeting sequences were ACAGTTTGCTCTCAAG GTG, TGTTCACACTGGATTACAA, and GCAGTACAGGCC TTTGGCA. Mouse Tulp3 shRNA targeting sequences were GCAAAACGTCCAACTACCT, GAGCTGGCTGCTATCTGTT, and TTAGAGGACTTTGCGTATA.

Cell line models

Pancreatic MIN6 β cells (passages 5–15) were a gift from Professor Jun-ichi Miyazaki (Department of Stem Cell Regulation Research, Graduate School of Medicine, Osaka University, Osaka, Japan). MIN6 and α-TC9 cells were cultured in DMEM medium containing 10% fetal bovine serum, 1 M HEPES, 50 mM 2-mercaptoethanol, 1% pen/strep, and 1% GlutaMAX.

Lentivirus production

Lentiviruses were produced by transient transfection of HEK293T cells with lentiviral vectors carrying the gene of interest and pMD2.G (Addgene 12259) and psPAX2 (Addgene 12260) packaging constructs. DMEM was replaced after overnight and virus was harvested 24, 48, and 72 h after transfection. Virus was filtered with a 0.45-mm OVDF filter (Millipore). Supernatants were collected and purified using PEG-it (System Biosciences). Concentrated lentivirus was stored at −80°C for transduction of primary human cells.

Cell line generation

To generate MIN6 and α-TC9 stable cell lines (passages <20), lentivirus carrying genes of interest were produced by cotransfecting 293T cells with pMD2.G, psPAX2, and pWPXLd/LAP-C/Puro-GPCRs plasmids previously described. Following infection for

48–72 h, cells were selected with either 10 µg/mL puromycin or sorting for GFP positive. To generate Crispr/Cas9 knockout cells, MIN6 and α-TC9 Cas9-BFP cells (passages <20) were infected with lentivirus containing the sgRNA of interest (sgGFP: GAC CAGGATGGGCACCACCC, and sgTulp3: GCGAAGGTT AAAGCCACG). Knockout efficiency was determined 10 d after infection by Western blotting. MIN6 and α-TC9 cells expressing Cas9-BFP were generated by infection of virus harvested from 293T cells transfected with p293 Cas9-BFP, pMD2.G, and psPAX2. MIN6 and α-TC9 Cas9-BFP cells were sorted for BFP positivity. For rescue experiments of MIN6 and α-TC9 sgRNA cells, the sgRNA was removed by adenoviral infection with recombinant Cre (Vector BioLabs 1060 and 1700), followed by sorting for GFP negativity.

Immunofluorescence staining

Cells were grown on 12-mm round coverslips and fixed with 4% paraformaldehyde (AlfaAesar 433689M) in PBS for 10 min at room temperature. Samples were blocked with 5% normal donkey serum (Jackson ImmunoResearch 017-000-121) in IF buffer (for FFAR4 staining: 3% BSA and 0.4% saponin in PBS; for all else: 3% BSA and 0.1% NP-40 in PBS) for 30 min at room temperature. Samples were incubated with primary antibody in IF buffer for 1 h at room temperature, followed by five washes with IF buffer. Samples were incubated with fluorescent-labeled secondary antibody for 30 min at room temperature, followed by a 5-min incubation with 4′,6-dia-midino-2-phenylindole (DAPI) in PBS for 5 min at room temperature and five washes with IF buffer. Coverslips were mounted with Fluoromount-G (SouthernBiotech 0100-01) onto glass slides followed by image acquisition. For the peptide blocking assay, the Ffar4 antibody was preincubated with a 20-fold molar excess of the immunizing peptide or an unrelated mock peptide for 3 h with rotation at room temperature immediately before primary antibody staining. The peptides used are described below. Antibodies used were as follows: FFAR4 (residues PILYNMSLFRNEWRK; 1:600) (Hilgendorf et al. 2019), FFAR4 (1:100; Santa Cruz Biotechnology sc-390752), acetylated tubulin (1:2000; Sigma T7451), PTGER4 (1:100; Santa Cruz Biotechnology sc-55596), KISS1R (1;500; a kind gift from Professor Kirk Mykytyn, The Ohio State University), ARL13B (1:1000; University of California at Davis/National Institutes of Health NeuroMab Facility 73-287), FGFR1OP (1:1000; Novus H00011116-M01), and GFP (1:2000; Invitrogen A10262).

Epifluorescence and confocal imaging

Images were acquired on an Everest deconvolution workstation (Intelligent Imaging Innovations) equipped with a Zeiss AxioImagerZ1 microscope and a CoolSnapHQ cooled CCD camera (Roper Scientific) and a 40× NA1.3 plan-apochromat objective lens (Zeiss 420762-9800) was used. Confocal images were acquired on a Marianas spinning disk confocal (SDC) microscopy (Intelligent Imaging Innovations). For Figure 2 and Supplemental Figure S2, images were acquired using a Leica DMi8 microscope equipped with a DFC7000T color camera (bright-field images) as well as the SPE confocal system (immunofluorescence).

Sample preparation and immunoblot

Cells were lysed in 1× LDS buffer containing DTT and incubated for 20 min at 95°C. Cells were lysed in RIPA buffer with protease inhibitors (50 mM Tris-HCl at pH 8.0, 150 mM NaCl, 1% NP-40, 20 mM β-glycerophosphate, 20 mM NaF, 1 mM Na_3VO_4, protease inhibitors including 1 µg/µL leupeptin, 1 µg/µL pepstatin,

and 1 μg/μL aprotinin) for 30 min at 4°C. The cell lysates were centrifuged at 16,000g for 15 min at 4°C. Proteins were separated using NuPage 4%–12% Bis-Tris gel (Thermo Fisher Scientific WG1402BOX) in NuPage MOPS SDS running buffer (50 mM MOPS, 50 mM TrisBase, 0.1% SDS, 1 mM EDTA at pH 7.7), followed by transfer onto PVDF membranes (Millipore IPFL85R) in transfer buffer (25 mM Tris, 192 mM glycine at pH 8.3) containing 10% methanol. Membranes were blocked in nonfat dry milk in PBS for 30 min at room temperature, followed by incubation with primary antibody in blocking buffer overnight at 4°C. The membrane was washed four times for 10 min in TBST buffer (20 mM Tris, 150 mM NaCl, 0.1% Tween 20 at pH 7.5) at room temperature, incubated with secondary IRDye antibodies (LI-COR) in blocking buffer for 1 h at room temperature, and then washed four times for 10 min in TBST buffer. Membranes were scanned on an Odyssey CLx imaging system (LI-COR), with protein detection at 680 and 800 nm. Antibodies used were as follows: TULP3 (1:2000; Yenzym) (Hilgendorf et al. 2019) and Tubulin (1:5000; Sigma 9026).

Quantitative real-time PCR

RNA was extracted using the RNeasy lipid tissue kit (Qiagen) and cDNA was synthesized using M-MLV reverse transcriptase (Invitrogen 28025-013). Quantitative real-time PCR was performed using TaqMan probes (Invitrogen) and the TaqMan gene expression master mix (Applied Biosystems 4369016) in 96-well Micro Amp optical reaction plates (Applied Biosystems N8010560). Expression levels were normalized to the average expression of the housekeeping gene. Probes used were Life Technologies TaqMan probe Tulp3 (Mm00495808_m1), TULP3 (Hs00163258_m1), Ffar4 (Mm00725193_m1), and Ptger4 (Mm00436053_m1).

Live cell ciliary cAMP assay

MIN6 and α-TC9 cells were seeded at 1×10^5 cells/well in a 96-well cell imaging plate (Eppendorf 0030741013) and transduced the following day with the ratiometric cilia-targeted cADDis Bac-Mam (Molecular Montana D0211G) according to the manufacturer's recommendation. Briefly, cells were infected with 25 μL of BacMam sensor stock in a total of 150 μL of medium containing 2 mM sodium butyrate (Molecular Montana) for overnight in a 37°C incubator. Prior to imaging, cells were incubated in PBS for 30 min at room temperature. Images were acquired on a Marianas spinning disk confocal (SDC) microscopy (Intelligent Imaging Innovations) (40×, epifluorescence) every 1 min for 15 min with agonist added after 30 sec. Red fluorescence was used to determine a mask and background subtracted green and red fluorescent intensity over time was determined using Slidebook (Intelligent Imaging Innovations).

In vitro insulin and glucagon secretion assays

MIN6 and α-TC9 (1×10^5) seeded in 96-well plates and batches of 25 pseudoislets were used for in vitro secretion assays. MIN6, α-TC9 cells, and pseudoislets were incubated at a glucose concentration of 2.8 mM or 7 mM for 60 min as an initial equilibration period. Subsequently, MIN6, α-TC9 cells, and pseudoislets were incubated at 1 mM, 2.8 mM, 7 mM, or 16.7 mM glucose concentrations with or without agonist for 60 min each. Pseudoislets were then lysed in an acid-ethanol solution (1.5% HCL in 75% ethanol) to extract the total cellular insulin or glucagon content. Secreted human insulin or glucagon in the supernatants and pseudoislet lysates were quantified using either a human insulin ELISA kit or glucagon ELISA kit (both from Mercodia). Secreted

insulin levels were divided by total insulin content and presented as a percentage of total insulin content; a similar method of data analysis was employed for glucagon secretion assays. All secretion assays were carried out in RPMI 1640 (Gibco) supplemented with 2% fetal bovine serum (HyClone) and the above-mentioned glucose concentrations.

Reagents and treatment

The concentrations of the following reagents are indicated in the legends for Figures 2, 3, 5, and 6 and Supplemental Figures S2–S6: ESI-09, RP-cAMP, compound 19a (CAY10598), Salbutamol, UDP-α-D-glucose, and Exendin-4, which were from Cayman Chemical; AZ13581837, which was purchased from AOBIOUS; TUG891 and TG424, which were purchased from Tocris; and kisspeptin-10, which was purchased from Santa Cruz Biotechnology. Small molecules or peptides were dissolved in DMSO (Sigma-Aldrich 276855), ESI-09, or RP-cAMP 30 min prior to agonist or vehicle addition. The following reagents were used at the indicated concentrations in Figures 3, 5, and 6, and Supplemental Figures S3 and S5: 100 μM TUG891, 1 μM CAY10598, 2 μM KP-10, and 100 nM TUG424. Small molecules were dissolved in DMSO (Sigma-Aldrich 276855).

Quantification and statistical analysis

Statistical analyses were performed in Microsoft Excel and GraphPad Prism. Most data are represented as mean ± standard derivation (SD) as specified in the figure legends. Sample size and number of repeated experiments are described in the legends. P value was determined using the two-tailed unpaired Student's t-test. The precise P-values are shown in the figures. $P < 0.05$ was considered statistically significant. All experiments were repeated three or four times (see figure legends) with similar results.

Competing interest statement

The authors declare no competing interests.

Acknowledgments

References

Arda HE, Li L, Tsai J, Torre EA, Rosli Y, Peiris H, Spitale RC, Dai C, Gu X, Qu K, et al. 2016. Age-dependent pancreatic gene regulation reveals mechanisms governing human β cell function. *Cell Metab* **23:** 909–920. doi:10.1016/j.cmet.2016 .04.002

Badgandi HB, Hwang SH, Shimada IS, Loriot E, Mukhopadhyay S. 2017. Tubby family proteins are adapters for ciliary trafficking of integral membrane proteins. *J Cell Biol* **216:** 743–760. doi:10 .1083/jcb.201607095

Bailey CJ. 2020. GIP analogues and the treatment of obesity-diabetes. *Peptides* **125:** 170202. doi:10.1016/j.peptides.2019 .170202

Campbell JE, Drucker DJ. 2015. Islet α cells and glucagon–critical regulators of energy homeostasis. *Nat Rev Endocrinol* **11:** 329–338. doi:10.1038/nrendo.2015.51

Cano DA, Murcia NS, Pazour GJ, Hebrok M. 2004. *Orpk* mouse model of polycystic kidney disease reveals essential role of primary cilia in pancreatic tissue organization. *Development* **131:** 3457–3467. doi:10.1242/dev.01189

Carboneau BA, Allan JA, Townsend SE, Kimple ME, Breyer RM, Gannon M. 2017a. Opposing effects of prostaglandin E₂ receptors EP3 and EP4 on mouse and human β-cell survival and proliferation. *Mol Metab* **6:** 548–559. doi:10.1016/j.molmet.2017 .04.002

Carboneau BA, Breyer RM, Gannon M. 2017b. Regulation of pancreatic β-cell function and mass dynamics by prostaglandin signaling. *J Cell Commun Signal* **11:** 105–116. doi:10.1007/ s12079-017-0377-7

Carracher AM, Marathe PH, Close KL. 2018. International Diabetes Federation 2017. *J Diabetes* **10:** 353–356. doi:10.1111/ 1753-0407.12644

Censin JC, Nowak C, Cooper N, Bergsten P, Todd JA, Fall T. 2017. Childhood adiposity and risk of type 1 diabetes: a Mendelian randomization study. *PLoS Med* **14:** e1002362. doi:10.1371/ journal.pmed.1002362

Croze ML, Guillaume A, Ethier M, Fergusson G, Tremblay C, Campbell SA, Maachi H, Ghislain J, Poitout V. 2020. Combined deletion of free fatty-acid receptors 1 and 4 minimally impacts glucose homeostasis in mice. *Endocrinology* **162:** bqab002. doi:10.1210/endocr/bqab002

Gentilella R, Pechtner V, Corcos A, Consoli A. 2019. Glucagon-like peptide-1 receptor agonists in type 2 diabetes treatment: are they all the same? *Diabetes Metab Res Rev* **35:** e3070. doi:10.1002/dmrr.3070

Gerdes JM, Christou-Savina S, Xiong Y, Moede T, Moruzzi N, Karlsson-Edlund P, Leibiger B, Leibiger IB, Östenson CG, Beales PL, et al. 2014. Ciliary dysfunction impairs β-cell insulin secretion and promotes development of type 2 diabetes in rodents. *Nat Commun* **5:** 5308. doi:10.1038/ncomms6308

Grarup N, Moltke I, Andersen MK, Dalby M, Vitting-Seerup K, Kern T, Mahendran Y, Jørsboe E, Larsen CVL, Dahl-Petersen IK, et al. 2018. Loss-of-function variants in ADCY3 increase risk of obesity and type 2 diabetes. *Nat Genet* **50:** 172–174. doi:10.1038/s41588-017-0022-7

Green WR. 1980. Abnormal cilia in human pancreas. *Hum Pathol* **11:** 686–687. doi:10.1016/S0046-8177(80)80085-2

Hearn T. 2019. ALMS1 and Alström syndrome: a recessive form of metabolic, neurosensory and cardiac deficits. *J Mol Med (Berl)* **97:** 1–17. doi:10.1007/s00109-018-1714-x

Hilgendorf KI, Johnson CT, Jackson PK. 2016. The primary cilium as a cellular receiver: organizing ciliary GPCR signaling. *Curr Opin Cell Biol* **39:** 84–92. doi:10.1016/j.ceb.2016.02.008

Hilgendorf KI, Johnson CT, Mezger A, Rice SL, Norris AM, Demeter J, Greenleaf WJ, Reiter JF, Kopinke D, Jackson PK. 2019. Omega-3 fatty acids activate ciliary FFAR4 to control adipogenesis. *Cell* **179:** 1289–1305.e21. doi:10.1016/j.cell .2019.11.005

Hodson DJ, Mitchell RK, Marselli L, Pullen TJ, Gimeno Brias S, Semplici F, Everett KL, Cooper DM, Bugliani M, Marchetti P, et al. 2014. ADCY5 couples glucose to insulin secretion in human islets. *Diabetes* **63:** 3009–3021. doi:10.2337/db13-1607

Hughes JW, Cho JH, Conway HE, DiGruccio MR, Ng XW, Roseman HF, Abreu D, Urano F, Piston DW. 2020. Primary cilia control glucose homeostasis via islet paracrine interactions. *Proc Natl Acad Sci* **117:** 8912–8923. doi:10.1073/pnas .2001936117

Ichimura A, Hasegawa S, Kasubuchi M, Kimura I. 2014. Free fatty acid receptors as therapeutic targets for the treatment of diabetes. *Front Pharmacol* **5:** 236. doi:10.3389/fphar.2014.00236

Ishihara H, Asano T, Tsukuda K, Katagiri H, Inukai K, Anai M, Kikuchi M, Yazaki Y, Miyazaki JI, Oka Y. 1993. Pancreatic β cell line MIN6 exhibits characteristics of glucose metabolism and glucose-stimulated insulin secretion similar to those of normal islets. *Diabetologia* **36:** 1139–1145. doi:10.1007/ BF00401058

Jiang JY, Falcone JL, Curci S, Hofer AM. 2019. Direct visualization of cAMP signaling in primary cilia reveals up-regulation of ciliary GPCR activity following Hedgehog activation. *Proc Natl Acad Sci* **116:** 12066–12071. doi:10.1073/pnas .1819730116

Jin D, Ni TT, Sun J, Wan H, Amack JD, Yu G, Fleming J, Chiang C, Li W, Papierniak A, et al. 2014. Prostaglandin signalling regulates ciliogenesis by modulating intraflagellar transport. *Nat Cell Biol* **16:** 841–851. doi:10.1038/ncb3029

Kluth O, Stadion M, Gottmann P, Aga H, Jähnert M, Scherneck S, Vogel H, Krus U, Seelig A, Ling C, et al. 2019. Decreased expression of cilia genes in pancreatic islets as a risk factor for type 2 diabetes in mice and humans. *Cell Rep* **26:** 3027–3036.e3. doi:10.1016/j.celrep.2019.02.056

Koemeter-Cox AI, Sherwood TW, Green JA, Steiner RA, Berbari NF, Yoder BK, Kauffman AS, Monsma PC, Brown A, Askwith CC, et al. 2014. Primary cilia enhance kisspeptin receptor signaling on gonadotropin-releasing hormone neurons. *Proc Natl Acad Sci* **111:** 10335–10340. doi:10.1073/pnas.1403286111

Legué E, Liem KF. 2019. Tulp3 is a ciliary trafficking gene that regulates polycystic kidney disease. *Curr Biol* **29:** 803. doi:10 .1016/j.cub.2019.01.054

Meloni AR, DeYoung MB, Lowe C, Parkes DG. 2013. GLP-1 receptor activated insulin secretion from pancreatic β-cells: mechanism and glucose dependence. *Diabetes Obes Metab* **15:** 15–27. doi:10.1111/j.1463-1326.2012.01663.x

Moore BS, Stepanchick AN, Tewson PH, Hartle CM, Zhang J, Quinn AM, Hughes TE, Mirshahi T. 2016. Cilia have high

cAMP levels that are inhibited by Sonic Hedgehog-regulated calcium dynamics. *Proc Natl Acad Sci* **113:** 13069–13074. doi:10.1073/pnas.1602393113

Moullé VS, Ghislain J, Poitout V. 2017. Nutrient regulation of pancreatic β-cell proliferation. *Biochimie* **143:** 10–17. doi:10.1016/j.biochi.2017.09.017

Mukhopadhyay S, Wen X, Chih B, Nelson CD, Lane WS, Scales SJ, Jackson PK. 2010. TULP3 bridges the IFT-A complex and membrane phosphoinositides to promote trafficking of G protein-coupled receptors into primary cilia. *Genes Dev* **24:** 2180–2193. doi:10.1101/gad.1966210

Nachury MV, Loktev AV, Zhang Q, Westlake CJ, Peränen J, Merdes A, Slusarski DC, Scheller RH, Bazan JF, Sheffield VC, et al. 2007. A core complex of BBS proteins cooperates with the GTPase Rab8 to promote ciliary membrane biogenesis. *Cell* **129:** 1201–1213. doi:10.1016/j.cell.2007.03.053

Nesmith JE, Hostelley TL, Leitch CC, Matern MS, Sethna S, McFarland R, Lodh S, Westlake CJ, Hertzano R, Ahmed ZM, et al. 2019. Genomic knockout of alms1 in zebrafish recapitulates Alström syndrome and provides insight into metabolic phenotypes. *Hum Mol Genet* **28:** 2212–2223. doi:10.1093/hmg/ddz053

Noguchi GM, Huising MO. 2019. Integrating the inputs that shape pancreatic islet hormone release. *Nat Metab* **1:** 1189–1201. doi:10.1038/s42255-019-0148-2

Östenson CG, Efendic S. 2007. Islet gene expression and function in type 2 diabetes; studies in the Goto-Kakizaki rat and humans. *Diabetes Obes Metab* **9:** 180–186. doi:10.1111/j.1463-1326.2007.00787.x

Peiris H, Park S, Louis S, Gu X, Lam JY, Asplund O, Ippolito GC, Bottino R, Groop L, Tucker H, et al. 2018. Discovering human diabetes-risk gene function with genetics and physiological assays. *Nat Commun* **9:** 3855. doi:10.1038/s41467-018-06249-3

Pietrzak-Nowacka M, Safranow K, Byra E, Nowosiad M, Marchelek-Myśliwiec M, Ciechanowski K. 2010. Glucose metabolism parameters during an oral glucose tolerance test in patients with autosomal dominant polycystic kidney disease. *Scand J Clin Lab Invest* **70:** 561–567. doi:10.3109/00365513.2010.527012

Powers AC, Efrat S, Mojsov S, Spector D, Habener JF, Hanahan D. 1990. Proglucagon processing similar to normal islets in pancreatic α-like cell line derived from transgenic mouse tumor. *Diabetes* **39:** 406–414. doi:10.2337/diab.39.4.406

Qiu L, LeBel RP, Storm DR, Chen X. 2016. Type 3 adenylyl cyclase: a key enzyme mediating the cAMP signaling in neuronal cilia. *Int J Physiol Pathophysiol Pharmacol* **8:** 95–108.

Ribeiro RA, Bonfleur ML, Batista TM, Borck PC, Carneiro EM. 2018. Regulation of glucose and lipid metabolism by the pancreatic and extra-pancreatic actions of taurine. *Amino Acids* **50:** 1511–1524. doi:10.1007/s00726-018-2650-3

Riddy DM, Delerive P, Summers RJ, Sexton PM, Langmead CJ. 2018. G protein-coupled receptors targeting insulin resistance, obesity, and type 2 diabetes mellitus. *Pharmacol Rev* **70:** 39–67. doi:10.1124/pr.117.014373

Robertson RP. 1988. Eicosanoids as pluripotential modulators of pancreatic islet function. *Diabetes* **37:** 367–370. doi:10.2337/diab.37.4.367

Sarchielli E, Comeglio P, Squecco R, Ballerini L, Mello T, Guarnieri G, Idrizaj E, Mazzanti B, Vignozzi L, Gallina P, et al. 2017. Tumor necrosis factor-α impairs kisspeptin signaling in human gonadotropin-releasing hormone primary neurons. *J Clin Endocrinol Metab* **102:** 46–56. doi:10.1210/jc.2016-2115

Shibasaki T, Sunaga Y, Seino S. 2004. Integration of ATP, cAMP, and Ca^{2+} signals in insulin granule exocytosis. *Diabetes* **53:** S59–S62. doi:10.2337/diabetes.53.suppl_3.S59

Sundström L, Myhre S, Sundqvist M, Ahnmark A, McCoull W, Raubo P, Groombridge SD, Polla M, Nyström AC, Kristensson L, et al. 2017. The acute glucose lowering effect of specific GPR120 activation in mice is mainly driven by glucagon-like peptide 1. *PLoS One* **12:** e0189060. doi:10.1371/journal.pone.0189060

Volta F, Scerbo MJ, Seelig A, Wagner R, O'Brien N, Gerst F, Fritsche A, Häring HU, Zeigerer A, Ullrich S, et al. 2019. Glucose homeostasis is regulated by pancreatic β-cell cilia via endosomal EphA-processing. *Nat Commun* **10:** 5686. doi:10.1038/s41467-019-12953-5

Zimmerman K, Yoder BK. 2015. SnapShot: sensing and signaling by cilia. *Cell* **161:** 692–692.e1. doi:10.1016/j.cell.2015.04.015

Discovery of ciliary G protein-coupled receptors regulating pancreatic islet insulin and glucagon secretion

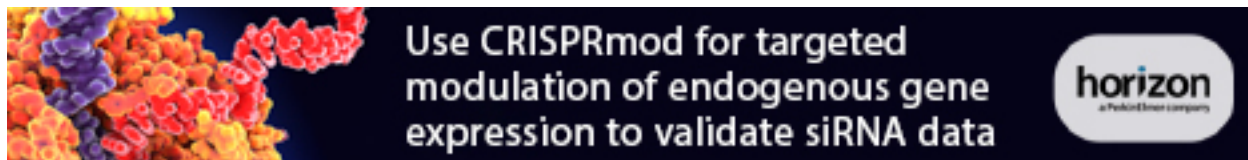Chien-Ting Wu, Keren I. Hilgendorf, Romina J. Bevacqua, et al.

Supplemental Material	http://genesdev.cshlp.org/content/suppl/2021/08/11/gad.348261.121.DC1
References	This article cites 46 articles, 11 of which can be accessed free at: http://genesdev.cshlp.org/content/35/17-18/1243.full.html#ref-list-1
Creative Commons License	This article is distributed exclusively by Cold Spring Harbor Laboratory Press for the first six months after the full-issue publication date (see http://genesdev.cshlp.org/site/misc/terms.xhtml). After six months, it is available under a Creative Commons License (Attribution-NonCommercial 4.0 International), as described at http://creativecommons.org/licenses/by-nc/4.0/.
Email Alerting Service	Receive free email alerts when new articles cite this article - sign up in the box at the top right corner of the article or **click here.**